INSTRUMENTATION OF REENTRY PLASMA EXPERIMENTS ON TRAIL-BLAZER II ROCKET A21.220-1

J. Spencer Rochefort, et al

Northeastern University

Prepared for:

Air Force Cambridge Research Laboratories

31 July 1974

AD/A002 375

MIL-STD-847A
31 January 1973

Unclassified

SECURITY CLASSIFICATION OF THIS PAGE (When Data Entered)

REPORT DOCUMENTATION PAGE	READ INSTRUCTIONS BEFORE COMPLETING FORM
1. REPORT NUMBER: AFCRL TR-74-0385	2. GOVT ACCESSION NO. / 3. RECIPIENT'S CATALOG NUMBER
4. TITLE (and Subtitle): INSTRUMENTATION OF REENTRY PLASMA EXPERIMENTS ON TRAILBLAZER II ROCKET A21.220-1	5. TYPE OF REPORT & PERIOD COVERED: Final-16 August 1971 30 June 1974 / 6. PERFORMING ORG. REPORT NUMBER
7. AUTHOR(s): J. Spencer Rochefort, Raimundas Sukys, Steven Goldberg	8. CONTRACT OR GRANT NUMBER(s): F19628-72-C-0050
9. PERFORMING ORGANIZATION NAME AND ADDRESS: Northeastern University, Electronics Research Laboratory, Boston, Ma. 02115	10. PROGRAM ELEMENT, PROJECT, TASK AREA & WORK UNIT NUMBERS: 4642-01-01, 62101F
11. CONTROLLING OFFICE NAME AND ADDRESS: Air Force Cambridge Research Laboratories (LZ), Hanscom AFB, Massachusetts 01730, Contract Monitor: Joseph L. Poirier/LZP	12. REPORT DATE: 31 July 1974 / 13. NUMBER OF PAGES: 39 / 15. SECURITY CLASS. (of this report): Unclassified / 15a. DECLASSIFICATION/DOWNGRADING SCHEDULE
16. DISTRIBUTION STATEMENT (of this Report): A-Approved for public release; distribution unlimited.	
17. DISTRIBUTION STATEMENT (of the abstract entered in Block 20, if different from Report)	
18. SUPPLEMENTARY NOTES: Tech., other	Reproduced by NATIONAL TECHNICAL INFORMATION SERVICE, US Department of Commerce, Springfield, VA. 22151
19. KEY WORDS (Continue on reverse side if necessary and identify by block number): Reentry Communications, Plasma Diagnostics, Electrostatic Probes, Ablation, Microwave Reflectometers.	

20. ABSTRACT (Continue on reverse side if necessary and identify by block number)

A Trailblazer II rocket was launched on December 6, 1973, from the NASA rocket test facility at Wallops Island, Virginia to study the properties of the shock-ionized flow field and its effects on microwave radiation. The reentry vehicle used an ablative, Teflon-coated nose cone to perform a plasma alleviation experiment. Instrumentation description is presented in

DD FORM 1 JAN 73 1473 EDITION OF 1 NOV 65 IS OBSOLETE

Unclassified

SECURITY CLASSIFICATION OF THIS PAGE (When Data Entered)

Unclassified

SECURITY CLASSIFICATION OF THIS PAGE(When Data Entered)

Block 20 Cont: this report.

The payload consisted of two primary microwave radiating and receiving test systems, a telemetry system which also served as a secondary test source, six fixed and two variable electrostatic probes, five nose cap ablation gauges and an accelerometer.

This report describes the design and operation of the electronic instrumentation which was fabricated for this reentry experiment. Included are circuit details of electrostatic probes, commutators, pulse slicers, four probe S-band field meters and various detector-amplifiers which were flown successfully in the experiment.

Unclassified

SECURITY CLASSIFICATION OF THIS PAGE(When Data Entered)

AFCRL-TR-74-0385

INSTRUMENTATION OF REENTRY PLASMA EXPERIMENTS ON TRAILBLAZER II ROCKET A21.220-1

J. Spencer Rochefort
Raimundas Sukys
Steven Goldberg

Northeastern University
Boston, Massachusetts 02115

Contract No. F19628-72-C-0050
Project No. 4642

ERRATA

On the cover page, the last line of the title should read, ON TRAILBLAZER II ROCKET A21.220-1, instead of the previously printed, ON TRAILBLAZER II ROCKET A21.200-1.

TABLE OF CONTENTS

LIST OF TABLES AND ILLUSTRATIONS

INTRODUCTION

A. TRAILBLAZER II PROGRAM SUMMARY

Whenever an aerospace vehicle reenters the earth's atmosphere at sufficient velocity to produce a shock-ionized field, problems are encountered in the transmission of signals at certain frequencies. Carried to the extreme, a complete communication blackout occurs when the electron concentration in the plasma sheath near an antenna reaches or exceeds a critical value which is dependent upon such factors as vehicle shape, velocity, altitude, antenna configuration and the transmission frequency.

The Air Force Cambridge Research Laboratory has been carrying out a research program to investigate and control the effects of reentry ionization on microwave antenna systems. In this program AFCRL has defined the experimental goals and has supplied the nose cones, microwave antennas, flush mounted diagnostic probes and has also been responsible for the reduction and analysis of the flight test data. Northeastern University has provided the electronic and microwave instrumentation systems required to achieve the program goals and also was responsible for the operation of the payloads during the flight test operations.

Five payloads have been launched. The first three vehicles measured the properties exhibited by the plasma formed during reentry and its effect on S-band transmissions.*[1-3] The fourth payload included liquid Freon 114B2 injection apparatus to alleviate the plasma by this electrophilic chemical process.[4] The fifth payload (produced under this contract) employed the ablation of a Teflon - covered nose cap as a source of electrophilic material. In this final approach the nose cone ablated as a result of the heat produced during reentry and released the additives into the flow prior to its passing over the antennas.

All the flights have been successful and the preliminary data analysis currently in process at AFCRL shows that the ablating Teflon was an effective plasma quenching agent.

---

*Numbered superscripts refer to the numbered references in the bibliography.

B. FINAL FLIGHT

This final payload was launched from the NASA Wallops Station test facilities at Wallops Island, Virginia, aboard Trailblazer A21.220-1 on December 6, 1973, at 22:59 Z hours. The first two stages of the rocket carried the nose cone to an apogee of approximately 322 kilometers. During the ascent the third stage X-248 motor and the nose cone which contained not only the instrumentation but also the fourth stage 39 centimeter spherical TEM-456 motor were enclosed in a protective shell and were facing down. Rexolite windows were located in the shell opposite all six transmitting antennas of the nose cone. This allowed for a continuous reception and monitoring of the telemetry and test signals during the ascent.

Shortly after lift-off the canted fins of the second stage motor induced a spin to stabilize the vehicle for the entire flight. At an altitude of approximately 77,700 meters the velocity package separated from the spent second stage motor and continued to cost up. After the apogee, when the vehicle began its descent, the third stage motor propelled the nose cone out of the protective shell. The final thrust was provided by the fourth stage spherical motor which remained inside the nose cone. The reentry began at approximately 91.5 kilometers with a velocity of 5,200 meters per second.

a The reentry vehicle was a blunt cone consisting of a 16.1 centimeter radius hemispherical nose cap and a nine degree half angle conical afterbody. The length of the nose cone measured along the center line was 67.23 centimeters and the base diameter was 48.69 centimeters. The skin of the nose cone was fabricated of aluminum and the nose cap was coated with Teflon. The antenna and probe locations of the reentry vehicle are tabulated in Table I. They are expressed as ratios of the distance S from the nose cap center point, measured along the surface of the vehicle, and the radius R of the nose cap. The angles are referenced to an arbitrary zero at the center of the low power S-band transmitting and receiving antennas and are measured clockwise looking into the tip of the nose cone.

C. PAYLOAD DESCRIPTION

The instrumentation was mounted on two plates in the forward section of the vehicle and in a number of tapered boxes on the inner surface of the nose cone. The weight of the instrumented nose cone, which included the spend fourth stage motor, was about 32 kilograms.

The payload consisted of two primary microwave radiating and receiving test systems, a telemetry system which served as a secondary test source, eight electrostatic probes and five ablation gauges imbedded into the material covering the nose cap. An accelerometer to monitor the changes in the vehicle motion was also included. Two separate power sources and controls were used for the instrumentation. The power distribution was separated into two networks: one for the telemetry system and the other for the test instruments. Both power packs consisted of 18 silver-zinc alkaline cells (Yardney PM-1) with an one ampere-hour capacity. Both batteries supplied over two amperes at 26.5 volts to the two systems, allowing slightly less than 30 minutes of operation on internal power. Since no recharging capability was provided, the payload was operated as much as possible on external power during testing and countdown.

S-band test systems were used to observe the effects of the plasma on antenna impedance mismatch and pattern distortion, interantenna coupling, signal attenuation and antenna voltage breakdown. The low power test system operated at 2290.5 MHz in CW mode with less than three watts of radiated power. The reflection coefficient of the test antenna was measured using reflectometer and four-probe field meter techniques. A measurement of mutual coupling was made between the transmitting test antenna and a receiving antenna located at S/R = 2.09 and S/R = 2.71 respectively. One of the telemetry antennas at S/R = 4.44 and $\theta = 285.5^{\circ}$ also was used as a secondary test antenna for reflectometer measurements.

The high power experiement operated at 2255.5 MHz in a pulsed mode. The antenna located at S/R = 2.09, $\theta = 180^{\circ}$ radiated approximately one kilowatt of peak power during each three microsecond pulse occuring at the rate of 160 pulses per second. A reflectometer was used to measure the reflected power. Sampling circuits were included to determine not only the magnitude of the reflected power but also to obtain approximate information as to when a voltage breakdown occurred during the pulse.

All of the antennas were designed and supplied by the Microwave Physics Laboratory of AFCRL. They were boron-nitride filled, cavity backed slots differing only in the dimensions necessary to accomodate the frequencies used. Figure 1 shows the components and the dimensions of the low power test antenna.

Eight flush mounted electrostatic probes were used to determine electron and ion densities near the surface of the nose cone. Six of the probes were supplied with a fixed bias, while two probes had their bias periodically switched between two levels. Locations of the various probes may be found in Table I.

Data was transmitted through a standard PAM/FM/FM S-band telemetry system operating at 2220.5 MHz. Four telemetry antennas were located at S/R = 4.44 equally spaced around the nose cone. A block diagram of the instrumentation is shown in Figure 2. Since this payload in many respects was similar to earlier instrumentation packages flown on Trailblazer II vehicles a more detailed information on the vehicle and on the general layout and packaging of the instruments may be found in reference 3.

CHAPTER I

LOW POWER INSTRUMENTATION

A. REFLECTOMETERS

Reflectometers were used to measure the magnitude of the power reflection coefficient at two antennas. One of the reflectometers measured the incident and the reflected powers at the main test antenna (S/R = 2.09, $\theta = 0^{o}$) while the other monitored one of the telemetry antennas (S/R = 4.44, $\theta = 285.5^{o}$). Both reflectometers used identical microwave components and differed only in the operating frequencies of the sources. Operational amplifiers were used to amplify the detected signals.

The block diagram describing the main S-band low power experiment is shown in Figure 3. The transmitter (Vector T-102S) operated at 2290.5 MHz and delivered nearly four watts of power at its output terminal. Insertion losses in the semirigid 0.358 cm cable and in other microwave components reduced the power at the test antenna to 2.85 watts. The choice of this relatively high power source for the experiment allowed the ground receiving stations to perform measurements of signal attenuation and antenna pattern distortion due to plasma.

The reflectometer consisted of a directional coupler (Narda 4013C-20) to monitor the incident power and a circulator (Amlabs GL-1024) which in conjunction with a 20 dB attenuator (Narda-4772-20) and a crystal detector (MA-462) measured the reflected power. The use of the circulator provided additional isolation for the transmitter and helped to keep the incident power constant during the reentry when large power reflections occurred. Since the circulator had 23 dB isolation between ports one and three and the incident power measurement was practically unaffected by the reflected power, the error in the measured power reflection coefficient was primarily due to the insufficient isolation of the circulator.[5] The maximum possible error at a given voltage reflection coefficient of the antenna was calculated from:

$$\epsilon_{\Gamma} = \frac{10^{-D/20}}{\Gamma} \times 100\% \qquad (1)$$

and is shown in Figure 4.

Where D is the effective isolation expressed in dB between ports one and three of the circulator and Γ is the actual voltage reflection coefficient.

B. MULTIPROBE FIELD METER

A four probe electric field meter was used to measure the phase of the reflection coefficient. The theory and the operation of such a device has been extensively discussed in various publications.[6-8] Only a very general description will be presented in this report.

The electric field meter was manufactured using stripline techniques. It consisted of fifty ohm transmission line and four equally spaced probes. The probes had approximately 23 dB of coupling and were terminated by Schottkey detector diodes. Quarter wave shorting stubs provided the dc return path The probes were calibrated by sequentially locating a peak of standing wave at each probe with a sliding short and then varying the incident power with a variable attenuator. The incident power was monitored through a directional coupler.

The detected output at each probe is related to the magnitude and the phase of the voltage reflection coefficient as:

$$P_n = V_n^2 = 1 + \rho^2 + 2\rho \cos(\theta - 2\varphi_n) \qquad (2)$$

Where ρ and θ are the magnitude and the angle of the coefficient and P_n is the effective power at that probe. The constant φ_n is the phase shift relating the distance of the probe to an arbitrary reference point along the transmission line. The phase may be calculated either from equation (2) using the magnitude of the reflection coefficient obtained from the directional coupler-isolator reflectometer or from the following equation:

$$\theta = \arctan - \frac{P_1 C'_{32} + P_2 C_{13} + P_3 C_{21}}{P_1 S_{32} + P_2 S_{13} + P_3 S_{21}} \qquad (3)$$

where P_1, P_2, and P_3 are the effective powers measured at three of the probes and:

$$C_{32} = \cos 2\varphi_3 - \cos 2\varphi_2$$

$$C_{13} = \cos 2\varphi_1 - \cos 2\varphi_3$$

$$C_{21} = \cos 2\varphi_2 - \cos 2\varphi_1$$

$$S_{32} = \sin 2\varphi_3 - \sin 2\varphi_2$$

$$S_{13} = \sin 2\varphi_1 - \sin 2\varphi_3$$

$$S_{21} = \sin 2\varphi_2 - \sin 2\varphi_1$$

If the magnitude of the reflection coefficient also has to be calculated from the probe data then:

$$(4) \qquad \rho = \left[\frac{1}{4P_I} \left(\left(P_1 C_{32} + P_2 C_{13} + P_3 C_{21} \right)^2 + \left(P_1 S_{32} + P_2 S_{13} + P_3 S_{21} \right)^2 \right) \right]^{1/2}$$

where P_I is the incident power in the line.

When probes are spaced one eighth of a wavelength apart the calculations may be simplified using:

$$(5) \qquad \theta = \arctan \frac{-P_1 + P_3}{P_1 + P_2 + P_3} + {}_mR$$

and

$$(6) \qquad \rho = \left[\frac{1}{4 P_I} \left(\left(P_1 - P_3 \right)^2 \quad \left(P_2 - P_4 \right)^2 \right) \right]^{1/2}$$

Since the arctan function refers the phase angle to the center probe (probe 2 in this case), ${}_mR$ is included to transfer the angle to any other convenient reference point.

C. MUTUAL COUPLING

The mutual coupling between the two test antennas at S/R = 2.09, $\theta = 0^o$ and S/R = 2.71, $\theta = 0^o$ was measured by detecting the received signal. The measured data included the effects of the continuously changing reflection coefficient of the transmitting antenna and the attenuation of the radiated singal as it propagated through plasma. Since the reflected power of the transmitting antenna was continuously monitored, separation of the two effects could easily be achieved during data reduction.

The measuring circuit consisted of an attenuator (Narda 4772-6), power monitor diode (MA-462) and a log-type amplifier. The amplifier shown in Figure 5 had a dynamic range exceeding four decades. The detected microwave signal was compressed by the silicon signal diode and the operational amplifier forming the log-type circuit. A dc return path was provided by the 6 dB attenuator used to reduce the coupled power into the crystal detector

to a safe operating level. Temperature compensation was achieved through the unity gain voltage follower circuit while gain and offset control was obtained from the output stage.

CHAPTER II

HIGH POWER EXPERIMENT

The high power experiment is indicated in the block diagram of Figure 2. Basically it involved a transmitter, reflectometer, and a specialized sample and hold system. The experiment consisted of the transmission of a three microsecond pulse of approximately one thousand watts peak power into the plasma sheath which exists around the nose cone during reentry into the atmosphere. Depending upon the ion concentration in the plasma, a portion of the pulse's power is reflected back into the antenna. If the concentration is high enough plasma breakdown can be expected, which manifests itself as a sudden increase in the pulse's reflected power.

The reflectometer needs little discussion because of its resemblance to units described in previous reports. The transmitter is triggered by means external to itself with the pulse width internally controlled. A slicer circuit was designed in order to satisfy bandwidth constraints. Because of the small width (three microseconds) and low repetition rate (one hundred sixty hertz) of the pulse, a prohibitive bandwidth would have been necessary for direct analog transmission of the pulse to the receiving station.

The slicer was developed to condition the reflected pulse for transmission with retention of as much information as possible. This was achieved by taking four samples from the pulse (located at 400, 750, 1600, 2600 nanoseconds from the leading edge) and displaying them for one half the time between pulses. The data therefore reveals the reflected power at specific times during the pulse and also shows if breakdown occurs sometime between sample times (once breakdown occurs it can be expected to remain until the pulse ends). The circuit is shown in Figure 7.

Two 160Hz unijunction clocks (one is shown in the lower left corner of the figure) are used as redundant triggering devices for the transmitter. They are capacitively coupled at point X for sycrhonized operation and connected at point Y to insure a trigger signal even if one clock should fail.

The incident transmitter pulse is monitored by a directional coupler (Figure 2). This signal is measured by the peak detector (upper left on Figure 7) and used as the initator for sampling the reflected pulse. The comparator used to detect the presence of a pulse is connected in parallel with the peak detector and actuated when one third the expected

voltage appears. The output signal from this device then actuates capacitively timed CMOS gates which sequentially open the switches between the reflected pulse amplifier and the holding capacitors (center of Figure 7). All switches are reset during the non-display period.

The reflected pulse is monitored by the reflectometer, amplified by an operational amplifier, and buffered by a bridge network to the holding capacitors (bottom center Figure 7). The second inverter of the sample logic provides the display signal for D-type flip-flops (top center of the same figure) which by capacitor timing sequentially turn on the FET switches shown at the right of the figure. These switches are driven by FET operational amplifiers which buffer the holding capacitors. The outputs from the switches are summed and amplified, and appear at the lower right of the figure. The output is therefore a piecewise approximation of the pulse with an expanded time frame. (The original 3 microsecond pulse is displayed for approximately 3 milliseconds).

CHAPTER III

ELECTROSTATIC PROBES

Eight flush mounted probes were flow as part of the payload to measure the ion density in the reentry plasma.[9] The probes supplied by AFCRL consisted of a 0.635 cm diameter goldplated copper electrode insulated from the vehicle by a cylindrical lava dielectric. The probe configuration is shown in Figure 6. The probes were provided with either positive voltage bias to measure electron density or negative voltage bias to obtain positive ion density measurements. Two of the probes, one for measuring the positive ion density and the other for measuring electron density, were provided with variable bias, while the rest were supplied with a fixed 15 volt bias.

A. FIXED BIAS PROBES

Four electron collecting and two positive ion collecting fixed bias probes were flown. A block diagram describing the general bias and the signal processing circuit arrangement designed and fabricated by Northeastern University is shown in Figure 8.

For each probe the 15 volt floating bias and the $\pm$ 15 volts required for the amplifiers were derived from a single transformer dc-dc converter. Rectification and filtering were achieved with standard four diode bridge circuits and capacitors. The floating bias supply had a monolythic - 723 regulator while the SG1501 dual unit provided the regulation for the signal processing circuits.

To accomodate four decades of probe current, logarithmic amplifiers were used. The current that was to be measured ranged from 100nA to 1mA for the positive ion probes and 1μA to 20mA for the electron probes. A common signal diode 1N4148 proved to be a rather good logarithmic element over that current range.

The logarithmic amplifier configuration may be seen in Figure 10 where the details of the probe circuits are shown. The dc-dc converter which was of standard design has been omitted for simplicity.

This configuration for the logarithmic amplifier instead of the more conventional one, where the log element is placed in the feedback loop, was chosen to minimize the influence of the converter noise. The path for the parasitic currents affecting the amplifier operation was provided by the floating bias supply and the dc-dc converter transformer winding capacitances.

When the floating supply and the probe were connected to the inverting input of the operational amplifier the noise tended to back-bias the log diode and produced very large noise spikes at the output of the amplifier at low probe currents. The usual type of compensation attempts, such as placing a capacitor across the log element and a resistance in series with the output of the operational amplifiers for stability, proved to be less effective than the configuration chosen. Floating the logarithmic amplifier instead of the bias supply, as was done in the switchable circuits, was avoided because of the common mode rejection complications with the available state of the art components at the time when the circuits were designed. One obvious disadvantage of the chosen configuration was a small variation of the probe bias voltage produced by the probe current flowing through the diode. To minimize this effect the bias supply voltage was increased such that the change in the probe bias was not larger than ± 250mV over the entire current range to be measured.

The temperature compensation of the log characteristic was acheived through a similar diode biased with a constant current and through a thermistor incorporated into the feedback loop of the logarithmic amplifier. The diode connected through a near unity gain amplifier compensated for the offset drift while the slope drift was controlled by the termistor-resistor network. Gain and offset adjustments were obtained from the output amplifier. A single point calibration and the assurance of a proper circuit operation prior to launch was obtained by grounding the calibrator input. This allowed a known current to flow through the resistor and the FET from the bias supply to ground simulating an operating probe.

The positive ion probes had similar circuits, but since the probe current flow was in a different direction the diodes, and of course, the bias supplies were reversed. The output amplifiers were connected in non-inverting configuration and the calibrating FET was replaced with its complement.

B. THE VARIABLE BIAS PROBES

A block diagram of a variable bias probe circuit is shown in Figure 11. The design was changed from the floating bias supply used in the fixed bias probe circuits to a floating logarithmic amplifier configuration. This accomplished a further reduction in the noise generated by the dc-dc converters. Also the dc-dc converter design was modified to a standard two transformer type.

The converters powered two ± 15 volt regulators (SG 1501) and a variable bias supply. One of the ± 15 volt units supplied power to the floating portion of the circuits, while the other provided power to the ground referenced circuits. The variable bias supply was switched between 15 and 30 volt levels by the digital control circuits which also controlled the probe data output format. To minimize the number of subcarries in the telemetry system, the data of the variable probes were transmitted in a NRZ-600 samples per second standard IRIG commutator format, where every third sample carried the data obtained from another fixed bias probe.[10]

A detailed circuit diagram of the electronics portion of the negative ion probe is shown in Figure 12. The dc-dc converter with the associated diode bridges and filtering capacitors as well as the ± 15 volt regulators which were the same as shown in figure 10 have been omitted for simplicity.

The UJT clock which drove the control logic circuits operated at a 600 pps rate. The sequence in the variable bias probe operation may be briefly described starting with a zero count stored in the decade/decimal output counters (-4017). This marked the beginning of the frame synchronization sequence with the output signal to the telemetry sitting at zero volts. The output of the SR flip-flop Q_1 was in the logical ONE state ($Q_1 = 1$) inhibiting the JK binaries (-4027) which were connected in the synchronous divide by three counter configuration. In this state $Q_3 = Q_4 = 0$. Since this forced the NOR gate output $G_3 = 0$, the analog (-4016) switches connecting the fixed and the variable probe data to the output amplifier were open. This state remained in effect until the seventh clock pulse when the decade counter reset Q_1 to zero signifying the end of the frame and the calibration period. During this interval the events at the data output were controlled by the counter through the status of Q_2 and the two NOR gates G_1 and G_2. The output was at the +5.0 volts when $G_2 = 1$. This occurred when the counter stored the counts of 1, 2, and 3 ($Q_2 = 1$, $G_1 = 0$) or when the counter contained the count of 6 ($Q_2 = 0$, $G_1 = 0$). At other times the amplifier output was at zero. With the seventh clock pulse the data period began in a sequence where first the data from the variable probe at the 15 volt bias level appeared at the output. This was followed by the data from the 30 volt bias level ($Q_3 = 1$) and, finally, the fixed probe data was connected to the output ($Q_3 = O$, $Q_4 = 1$). The presentation of data in this sequence continued until the counter read 60. At that point the counter reset and once again the frame synchronization sequence began.

The sequence of 15V - 30 V - fixed data was chosen to allow the longest possible reverse recovery time for the circuits. Every time the bias of the probe was changed, the capacitance associated with the cable leading from the diode to the probe had to be recharged. When the probe bias was increased the log diode became forward bias and the recharging took place through a relatively low impedance. However, returning the probe bias to a lower level back biased the diode and the recharging of the cable capacitance took place through a very high impedance. For this reason the output of the bias supply was changed from 30 to 15 volts at the same time when the analog gate was switched to transmit the fixed probe data allowing as long as possible for recharging of the cable capacitance. To speed up the recovery a restoration circuit was included which shunted a resistor across the probe every time the bias supply was returning to the 15 volt level. The same resistor was used for one point pre-flight calibration of the probe.

Since the logarithmic amplifier was floating, a common mode rejection circuit was used to bring the voltage levels within the range of the output operational amplifier. The output of the logarithmic amplifier was isolated by a unity gain amplifier from the voltage divider network. This was necessary to eliminate a relatively low resistance path which allowed a current to flow from the variable bias supply through the feedback resistance of the logarithmic amplifier and the voltage divider to ground.

Positive ion variable bias probe circuits were similar to the ones described. Besides the usual reversal of the log diode and the bias supply connections to accomodate the different direction of current flow, a FET input operational amplifier was used to amplify the diode voltage. Connections of the common mode circuit output amplifier were reversed to produce a positive output signal and the complement of the calibration transistor was used. The variable bias control circuit was more significantly modified and therefore is shown in Figure 9..

CHAPTER IV

TELEMETRY SYSTEM

A. CHANNEL ASSIGNMENT

Flight data were transmitted through a S-band PAM/FM/FM telemetry system. A standard IRIG proportional bandwidth subcarrier system was used. The subcarrier and the commutator channel assignments are given in Table II.

The transmitter (Vector T-105S) operated at 2220.5MHz providing each of the four telemetry antennas with approximately one watt of power. The antennas were boron-nitride filled cavity backed slots mounted near the base of the nose cone. At this location the effects of the plasma sheath on the transmitted signal were minimized. The power to the antennas was supplied through a matched four way power divider. To avoid re-distribution of power due to mismatches at the antennas during reentry, isolators were provided for three antennas. The fourth antenna was used as a secondary S-band test system where the magnitude of the reflection coefficent was measured. The reflectometer consisted of one directional coupler to measure incident power followed by a circulator which served the dual purpose of providing isolation for that antenna as well as diverting the reflected power into a detector for measurements.

The subcarrier system consisted of eleven subminiature voltage controlled oscillators (Vector MM0-11). Data signals were restricted to the zero to five volt range which produced ± 7.5 percent deviation from the subcarrier center frequency. Three of the channels were used for commutated data while the rest carried continuous signals. All commutated data associated with direct measurements of plasma parameters were sampled between 180 and 240 times per second. This ensured at least 15 data samples during each revolution of the reentering nose cone. Other parameters such as incident power measurements obtained from the reflectometers, ablation gauge and the accelerometer outputs were sampled less often. All three commutator outputs had the standard IRIG NRZ format. The two units which sampled only the electrostatic probe data had a ten frame per second rate, while the other commutator was running at thirty frames per second. Each unit produced sixty samples per frame including the synchronization and calibration segments.

Since this telemetry system in many respects was very similar to the telemetry systems flow on earlier Trailblazer rockets only a general description has been given. A more detailed discussion including the signal strength, the antenna pattern and the plasma effect considerations may be found in references 3, 11, 12.

B. COMMUTATOR INSTRUMENTATION

A special purpose commutator primarily designed to transmit data obtained from four of the fixed bias electrostatic probes and the five ablation gauges was flown. The output of the unit had a NRZ 60 segments per frame format and was operating at 30 frames per second. Five of the segments were assigned to produce the IRIG recommended frame synchronization pattern, while the first three segments following the frame synchronization supplied the calibration data in a zero-full scale-zero sequence. The next 52 segments were assigned to various data sources.

Twenty six data gates were connected in sequence to the output amplifier twice during each frame such that segments 4 through 29 carried data from the same sources and in the same sequence as segments 30 through 55. In this arrangement only eight CMOS-4016 analog gate packages were required to produce the whole frame, including synchronization. The number of the analog gates could have been further reduced since during the same half of the data sequence duplicate gates were assigned to transmit information from some of the same sources. A penalty for such a reduction in the number of the analog gates would have been an increased complexity of the control logic resulting into a larger size of the commutator package.

The circuit diagram of the commutator is shown in Figure 13. The analog gates connected to the data sources are shown as switches in two groups of ten and one group of six. In each group the switches having the same subscripts were controlled by the status of the decade/decimal output counter C_1 (-4017) terminals with corresponding numbers. The four switches marked by the double letters selected which of the groups would transmit data to the output. Group A transmitted when $Q_2 = 0$ and counter C_2 indicated zero count (ONE in the "0" position). After ten clock pulses C_2 indicated count of one and the B-group transmitted, then the C-group was connected to the output. After 26 clock pulses a rest pulse was generated at Q_3 which reset both decade counters

and advanced the divide by three counter (-4027). The D-type binary Q_3 was connected to produce a monostable operation. The time delay was obtained from the 1.5M resistor and the stray capacitance at the reset terminal R. Once reset the gating sequence repeated until once again a reset pulse was generated. At this time $Q_2 = 1$ and the switch DD connected the frame synchronization and calibration circuits to the buffer amplifier. Since $Q_4 = 0$ switch F_5 was open and switch F_0 was closed producing zero volts at the output and marking the beginning of the frame synchronization sequence. After the next clock pulse $Q_4 = 1$ and F_5 was closed ($F_0 = \overline{F}_5$) producing and holding +5.0 volts during the next three clock periods. The transistor Q_5 saturated during the fourth clock period and +2 volts appeared at the output. The fifth clock pulse reset Q_4 and produced zero calibration while the next pulse once again produced + 5.0 volts for the full scale calibration. The following clock pulse returned the output to zero and presented a logical ONE to the D input of Q_3 paving the way for a reset pulse coinciding with the next clock pulse. Now the data sequence repeated.

The clock pulses were generated by the UJT relaxation oscillator. Calibration voltage was derived using the-723 monolithic voltage regulator.

The commutator package also included the ablation gauge bias circuits. The gauges consisted of four resistance wires connected in parallel and imbedded at different depths into Teflon plugs which in turn were installed into the ablation cover of the nose cap. The wire closest to the surface had a nominal resistance of 275 ohms. The other resistances were 2.6k, 5.2k, and 8.5k at increasing depths, respectively. Each gauge was connected to +15 volt commutator supply, through a voltage divider consisting of 6.8k and 3.3k resistors going to the supply and ground respectively. When all wires were intact approximately 0.5 volts were produced at the output. A break in the wire closest to the surface increased the output to approximately two volts. Each additional break produced one volt increment with a maximum possible output of five volts when all wires were broken.

BIBLIOGRAPHY

1. J.S. Rochefort, L. J. O'Connor, C.H. Price, Jr., and R. Sukys, "Data Transmission and Trajectory Determining Devices For Research Rockets and Satellities", Final Report, Contact No. AF19(604)-3506, 30 June 1963.
2. J.S. Rochefort, L.J. O'Connor, R. Sukys and A. Glazer, "Data Transmission and Instrumentation for Space Vehicles", Final Report, Contract No. AF19(628)-2433, 30 April 1967.
3. J.S. Rochefort, R. Sukys, and R. Symmes, "Instrumentation and Flight Results of Reentry Plasma Diagnostic and Alleviation Experiments on Trailblazer II Rockets", Final Report, AFCRL-72-0695, Contract No. F19628-69-C-0150, Northeastern University Boston, Massachusetts October 1972.
4. J.F. Lennon and S.B. Herskovitz, "Design and Testing of a Chemical Injection System for Reentry Plasma Alleviation" AFCRL-TR-74-0113, February 28, 1974.
5. T. Mukaihata, M.F. Bottjer, and H.J. Tondreau, "Rapid Broad-Band Directional Coupler Directivity Measurements", IRE Transactions on Instrumentation, Vols. 1-9, No. 2, September 1960.
6. R. Caldecott, "Multiprobe Reflectometer and its Applications to Automated Transmission Line Measurements", submitted for publication in the IEEE Transactions for G-AP, July, 1972.
7. P. Bohley, R. Caldecott, R. McGown, and R.C. Taylor, "Measuring Missile Antenna Impedance in Flight", Electronics, 36, No. 28, July 12, 1963.
8. W.L. Grantham, "Flight Results of a 25,000 Foot-Per-Second Reentry Experiment Using Microwave Reflectometers to Measure Plasma Electron Density and Standoff Distance", NASA Technical Note, NASA TND-6062, Langley Research Center, Hampton, Virginia December 1970.
9. D.T. Hayes, "Electrostatic Probe Measurements of Flow Field Characteristics of a Blunt Body Reentry Vehicle", presented at the AIAA 5th Fluid and Plasma Dynamics Conference, Boston, Massachusetts. June 1972.

10. "Telemetry Standards" IRIG, Document 106-73. May 1973
11. L.J. Poirier, W. Rotman, D.T. Hayes, and J.F. Lennon, "Effects of Reentry Plasma Sheath on Microwave Antenna Performance: Trailblazer II Rocket Results of 18 June 1967", Report No. AFCRL-69-0354, U.S. Air Force Cambridge Research Laboratories August 1969.
12. D.T. Hayes, S.B. Herskovitz, J.F. Lennon, L.J. Poirier, "Preliminary Report on the Trailblazer II Chemical Alleviation Flight of 28 July, 1972", Report No. AFCRL-72-0640, U.S. Air Force Cambridge Research Laboratories. October 1972.

PERSONNEL

A list of the engineers and student assistants who contributed to the work reported is given below:

J. Spencer Rochefort, Professor of Electrical Engineering, Principal Investigator.

Raimundas Sukys, Senior Research Associate, Engineer.

Ronald Symmes, Research Assistant, Engineer.

Steven Goldberg, Research Assistant, Engineer.

Gerald O'Regan, Project Assistant

Thomas Palasek, Project Assistant

Jonathan Pearce, Project Assistant

RELATED CONTRACTS AND PUBLICATIONS

AF19(604)-3506	1 April 1958 through 30 June 1963
AF19(628)-2433	1 April 1963 through 31 March 1967
AF19(628)-5110	1 September 1965 through 28 February 1969
F19628-69-C-0150	1 March 1965 through 31 August 1972
F19628-72-C0050	16 August 1971 through 30 June 1974

J.S. Rochefort, L.J. O'Connor, C.H. Price, Jr., and R. Sukys, "Data Transmission and Trajectory Determining Devices for Research Rockets and Satellities", Final Report, Contract No. AF19(604)-3506. 30 June 1963.

J.S. Rochefort, L. J. O'Connor, R. Sukys and A. Glazer, "Data Transmission and Instrumentation Systems for Space Vehicles", Final Report Contract No. AF19(628)-2433, 30 April 1967.

J.S. Rochefort, R. Sukys, and R. Symmes "Instrumentation and Flight Results of Reentry Plasma Diagnostic and Alleviation Experiments on Trailblazer II Rockets", Final Report, Contract No. F19628-69-C-0150, 31 October 1972.

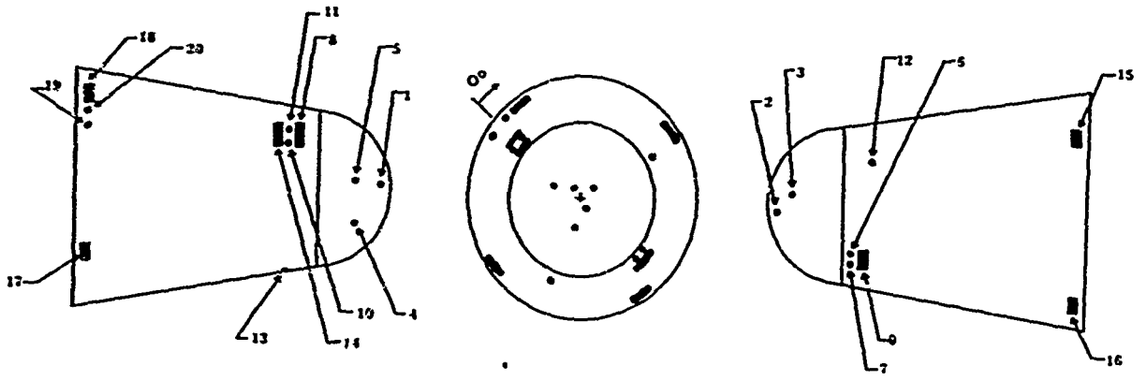

No	Device		S/R	θ
1	Ablation gauge-1		.18	15.0°
2	Ablation gauge-2		.18	195.0°
3	Ablation gauge-3		.48	105.0°
4	Ablation gauge-4		.79	225.0°
5	Ablation gauge-5		.79	345.0°
6	Electrostatic probe-4	Positive fixed bias	1.77	175.5°
7	Electrostatic probe-5	Negative fixed bias	1.77	184.5°
8	Test antenna	Low power, transmitting	2.09	0.0°
9	Test antenna	High power, transmitting	2.09	180.0°
10	Electrostatic probe-1	Positive variable bias	2.4	355.5°
11	Electrostatic probe-2	Negative variable bias	2.4	4.5°
12	Electrostatic probe-3	Positive fixed bias	2.4	111.0°
13	Electrostatic probe-6	Positive fixed bias	2.4	249.0°
14	Test antenna	Low power, receiving	2.71	0.0°
15	Telemetry antenna-1		4.44	105.5°
16	Telemetry antenna-2		4.44	195.5°
17	Telemetry antenna-3		4.44	285.5°
18	Telemetry antenna-4	Reflectometer	4.44	15.5°
19	Electrostatic probe-7	Positive fixed bias	4.44	355.5°
20	Electrostatic probe-8	Negative fixed bias	4.44	4.5°

TABLE I ANTENNA AND PROBE LOCATIONS

SUBCARRIERS

Band	Center Frequency	Data	Device
7	2.3 kHz	Reflected power	Test antenna
8	3.0 kHz	Coupled power	Test antenna
9	3.9 kHz	Probe 1 output	Field meter
10	5.4 kHz	Probe 2 output	Field meter
11	7.35 kHz	Probe 3 output	Field meter
12	10.5 kHz	Probe 4 output	Field meter
13	14.5 kHz	Reflected power	Telemetry antenna
16	40.0 kHz	Electron current	Commutator ES-2
17	52.5 kHz	Positive ion current	Commutator ES-1
19	93.0 kHz	Reflected power	High power antenn
20	124.0 kHz	Ion and electron current	Commutator

COMMUTATOR

Channels	Data	Device
1-3	Zero Calibration	
2	Full Scale Calibration	
4-11-18..37-44-51	Electron current	ES-3, S/R=2.4, $\theta = 111^{o}$
5-12-19..38-45-52	Electron current	ES-6, S/R=2.4, $\theta = 249^{o}$
6-13-20..39-46-53	Positive ion current	ES-8, S/R=4.44, $\theta = 355.5^{o}$
7-14-21..33-40-47	Electron current	ES-7, S/R=4.44, $\theta = 4.5^{o}$
8-24-34-50	Incident power	High power
9-35	Incident power	Telemetry antenna
10-36	Incident power	Test antenna
15-41	Ablation	Gauge S/R= .18, $\theta = 195.5^{o}$
16-42	Ablation	Gauge S/R= .18, $\theta = 15.0^{o}$
17-43	Ablation	Gauge S/R= .48, $\theta = 105.0^{o}$
22-48	Ablation	Gauge S/R= .79, $\theta = 225.0^{o}$
28-49	Ablation	Gauge S/R= .79, $\theta = 345.0^{o}$
29-55	Vehicle motion	Accelerometer

TABLE II TELEMETRY CHANNEL ASSIGNMENTS

COMMUTATOR ES-1

Channel	Data	Device
1	Zero calibration	
2	Full scale calibration	
3-6-9..48-51-54	Electron current 15 V variable bias	ES-1,S/R = 2.4, θ = 355.5^{o}
4-7-10..49-52-55	Electron current 30 V variable bias	ES-1,S/R = 2.4, θ = 355.5^{o}
5-8-11..47-50-53	Electron current, fixed bias	ES-4,S/R = 2.4, θ = 175.5^{o}

COMMUTATOR ES-2

Channel	Data	Device
1	Zero calibration	
2	Full scale calibration	
3-6-9..48-51-54	Positive ion current. -15 V variable bias	ES-2, S/R = 2.4, θ = 4.5^{o}
4-7-10..49-52-55	Positive ion current. -30V variable bias	ES-2, S/R = 2.4, θ = 4.5^{o}
5-8-11..47-50-53	Positive ion current. Fixed bias	ES-5, S/R = 2.4, θ = 184.5^{o}

TABLE II TELEMETRY CHANNEL ASSIGNMENTS (CONT.)

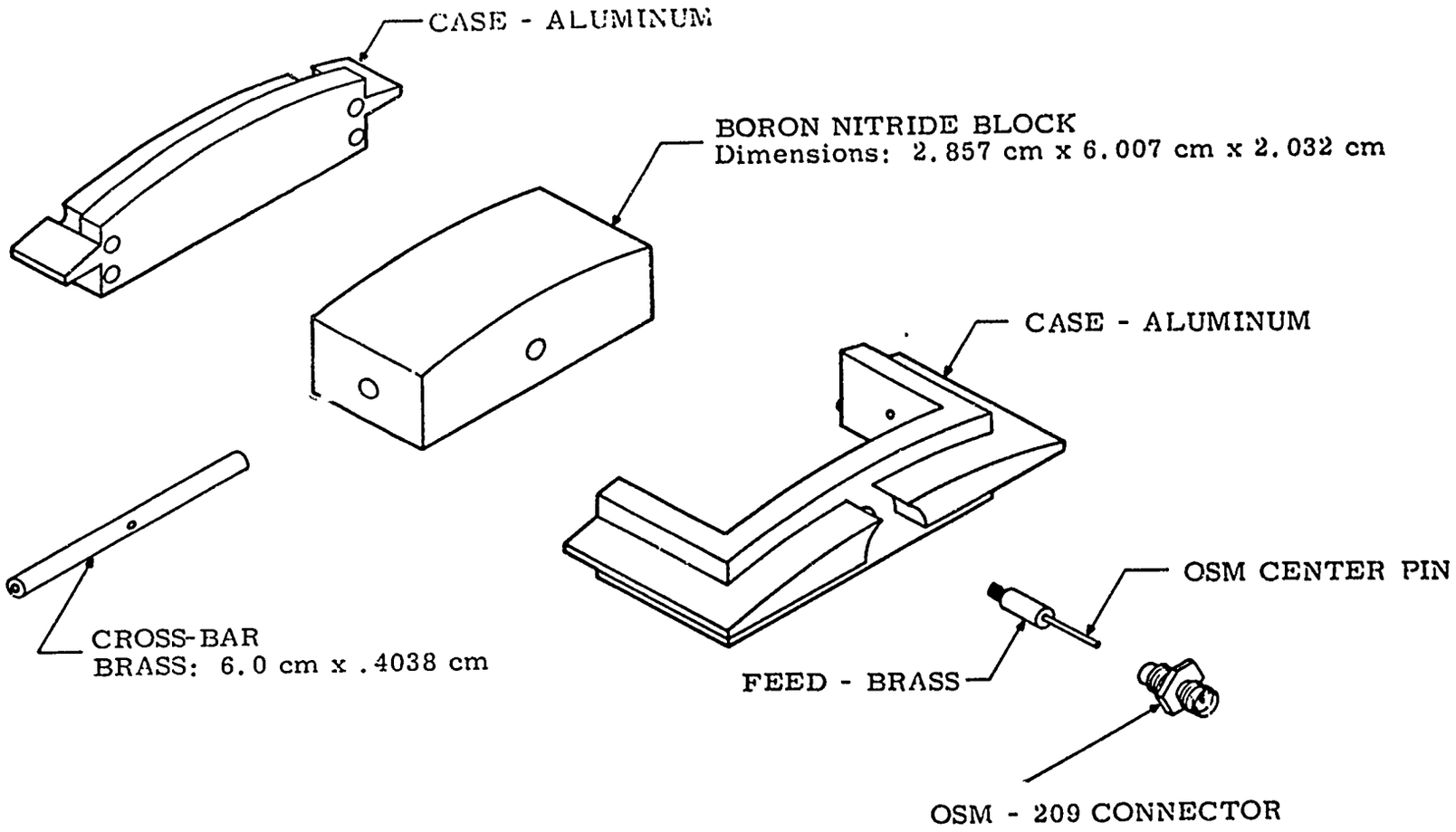

FIGURE 1 TEST ANTENNA

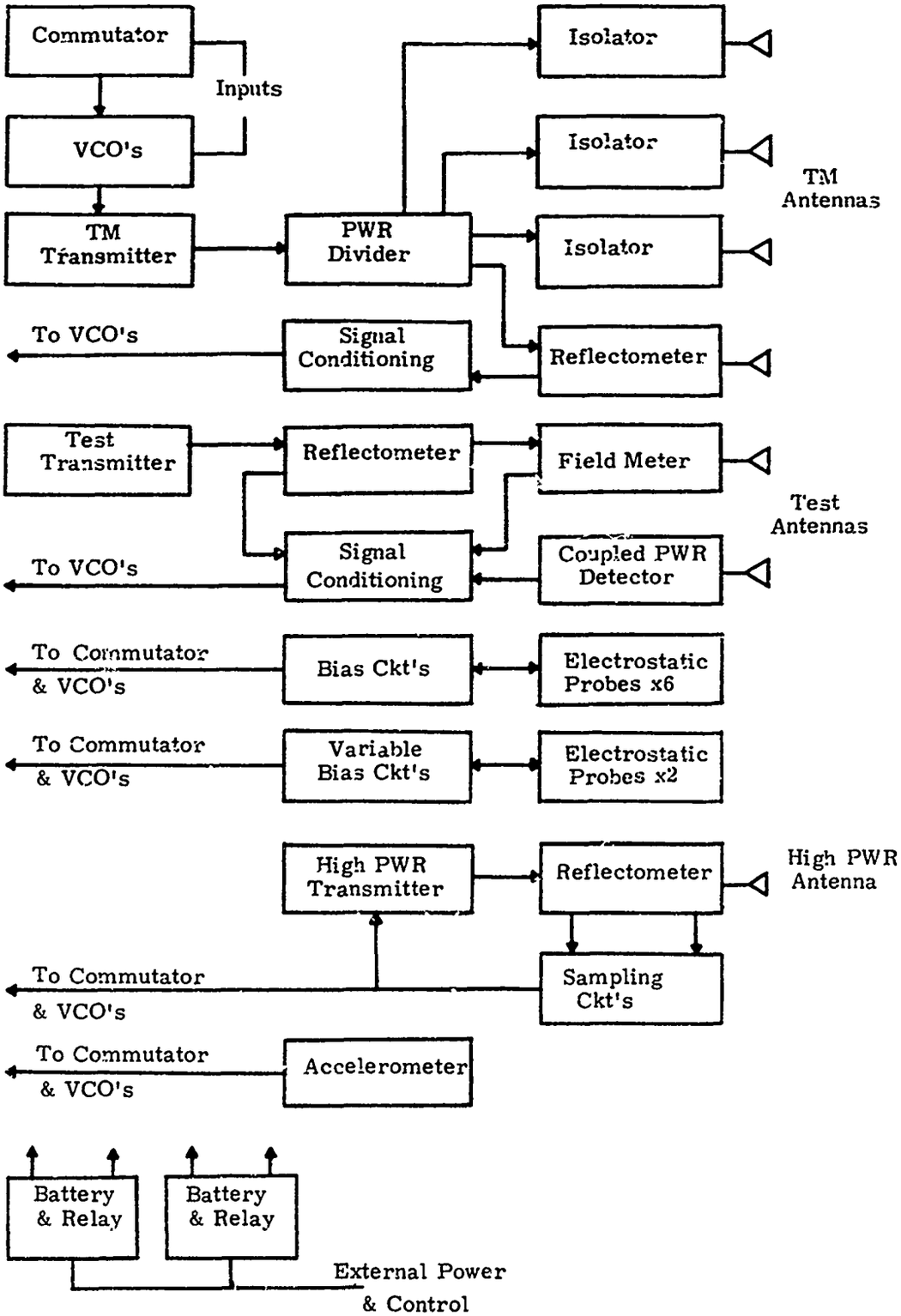

FIGURE 2 INSTRUMENTATION BLOCK DIAGRAM

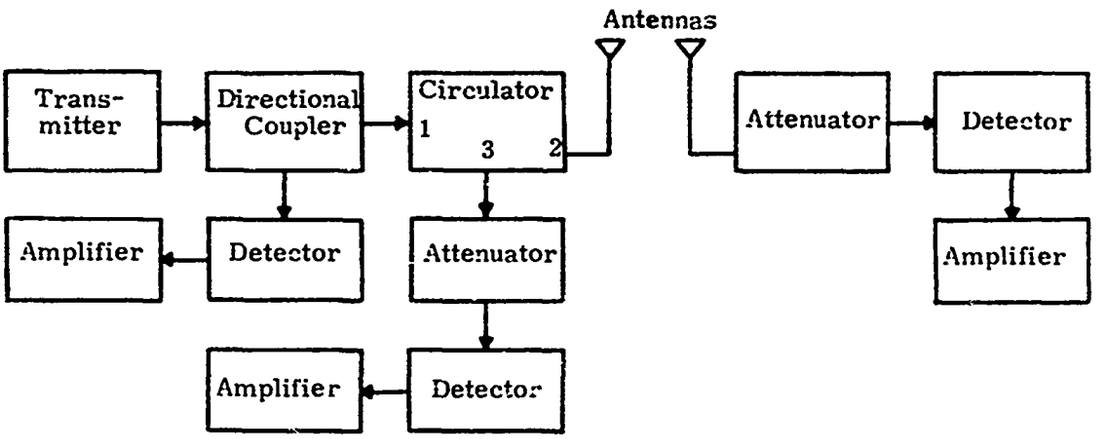

FIGURE 3 S-BAND EXPERIMENT BLOCK DIAGRAM

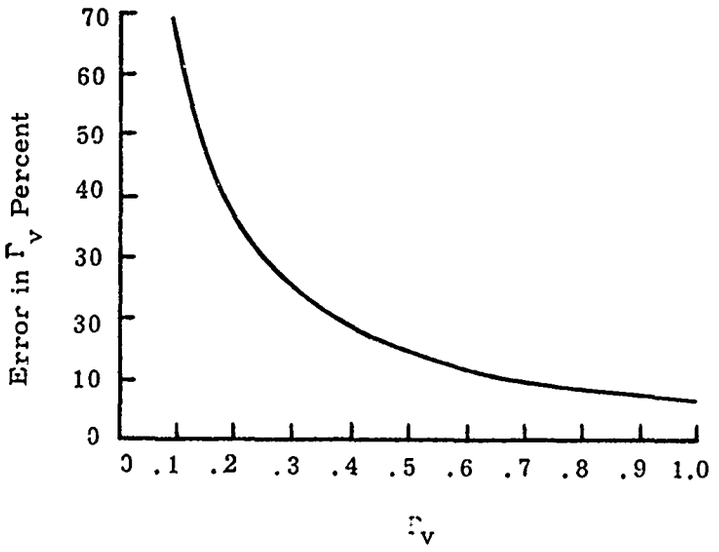

FIGURE 4 ERROR IN MEASURED REFLECTION COEFFICIENT

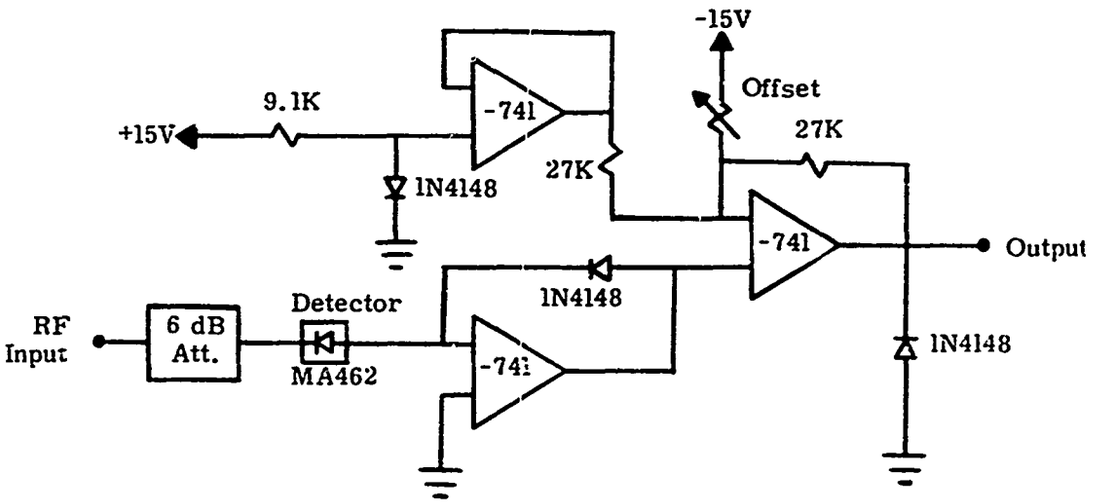

FIGURE 5 COUPLED SIGNAL AMPLIFIER

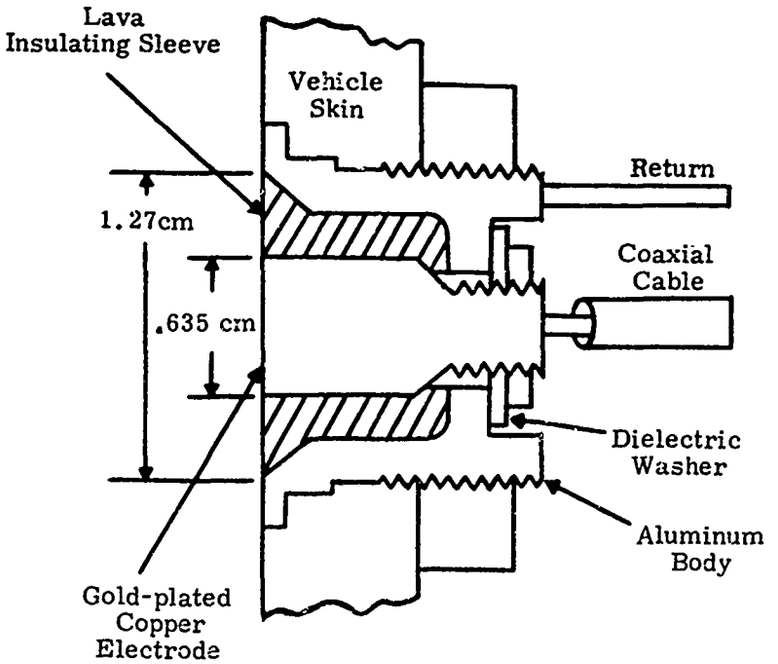

FIGURE 6 ELECTROSTATIC PROBE

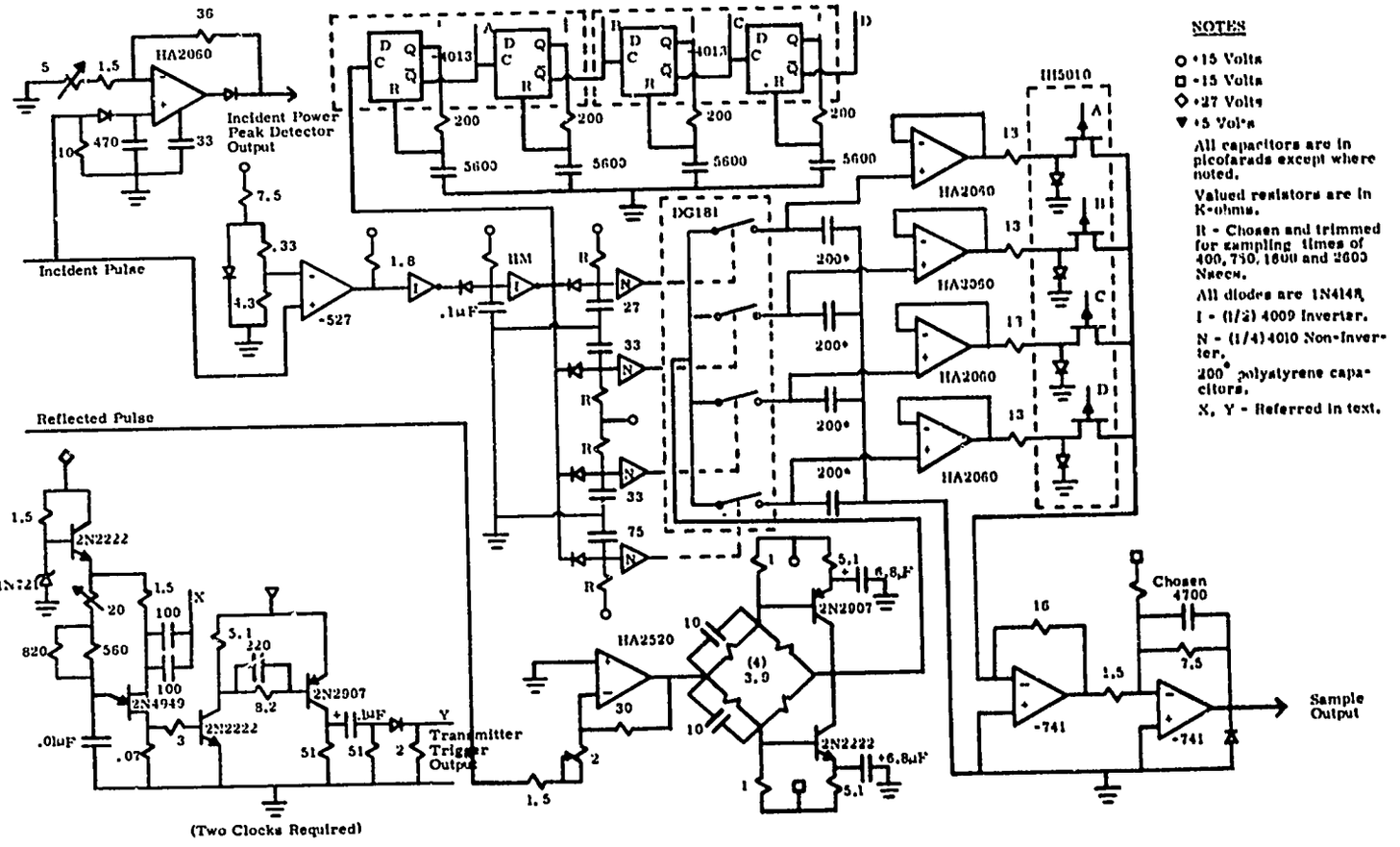

FIGURE 7 SAMPLE AND HOLD CIRCUITS

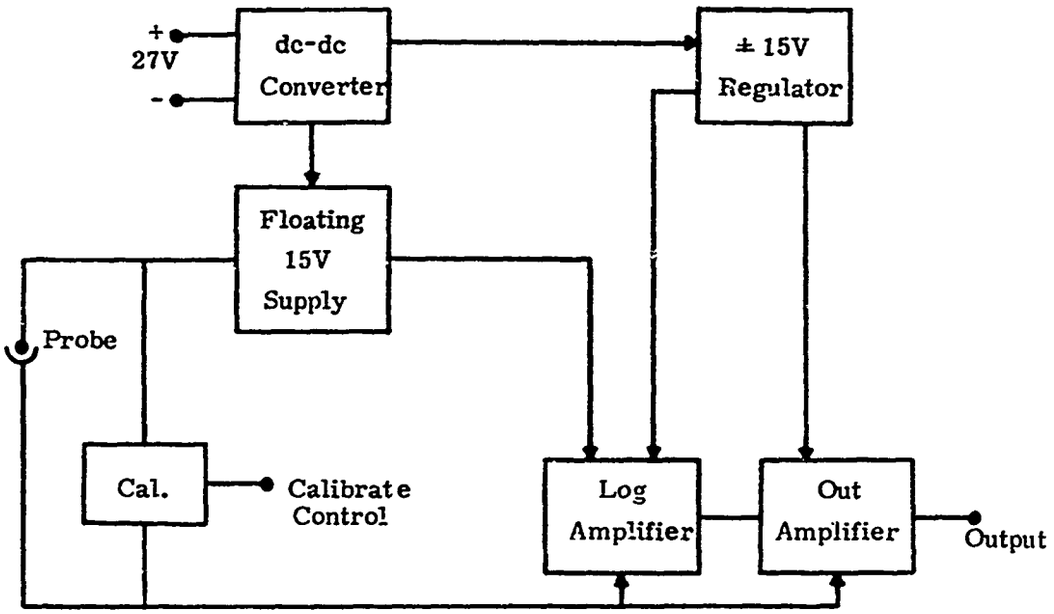

FIGURE 8 FIXED BIAS ES-PROBE DIAGRAM

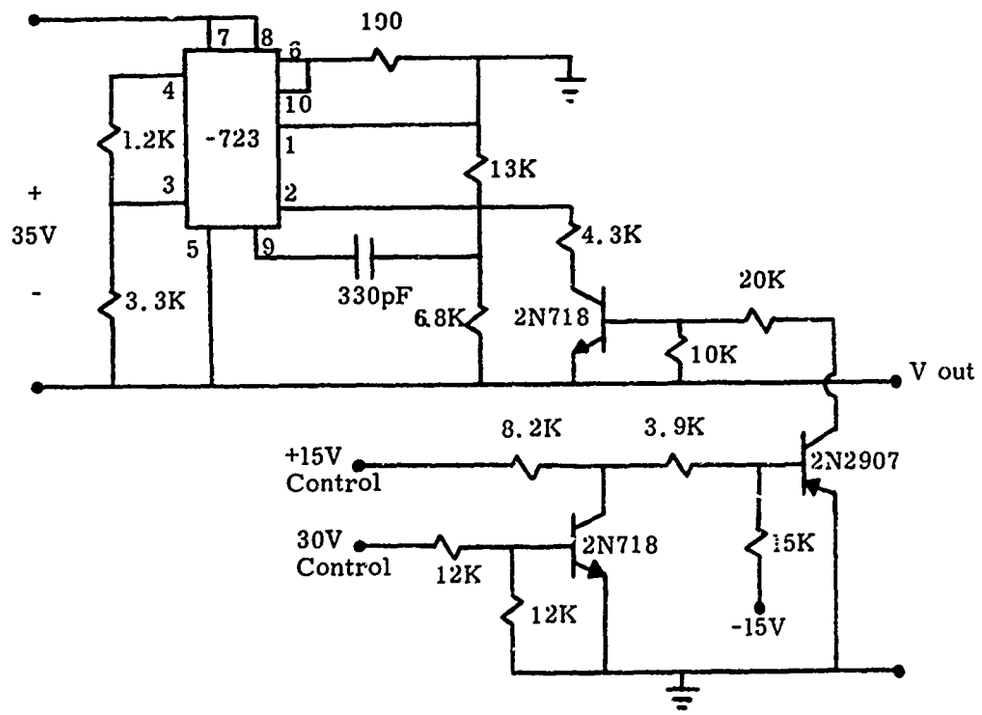

FIGURE 9 VARIABLE NEGATIVE VOLTAGE REGULATOR

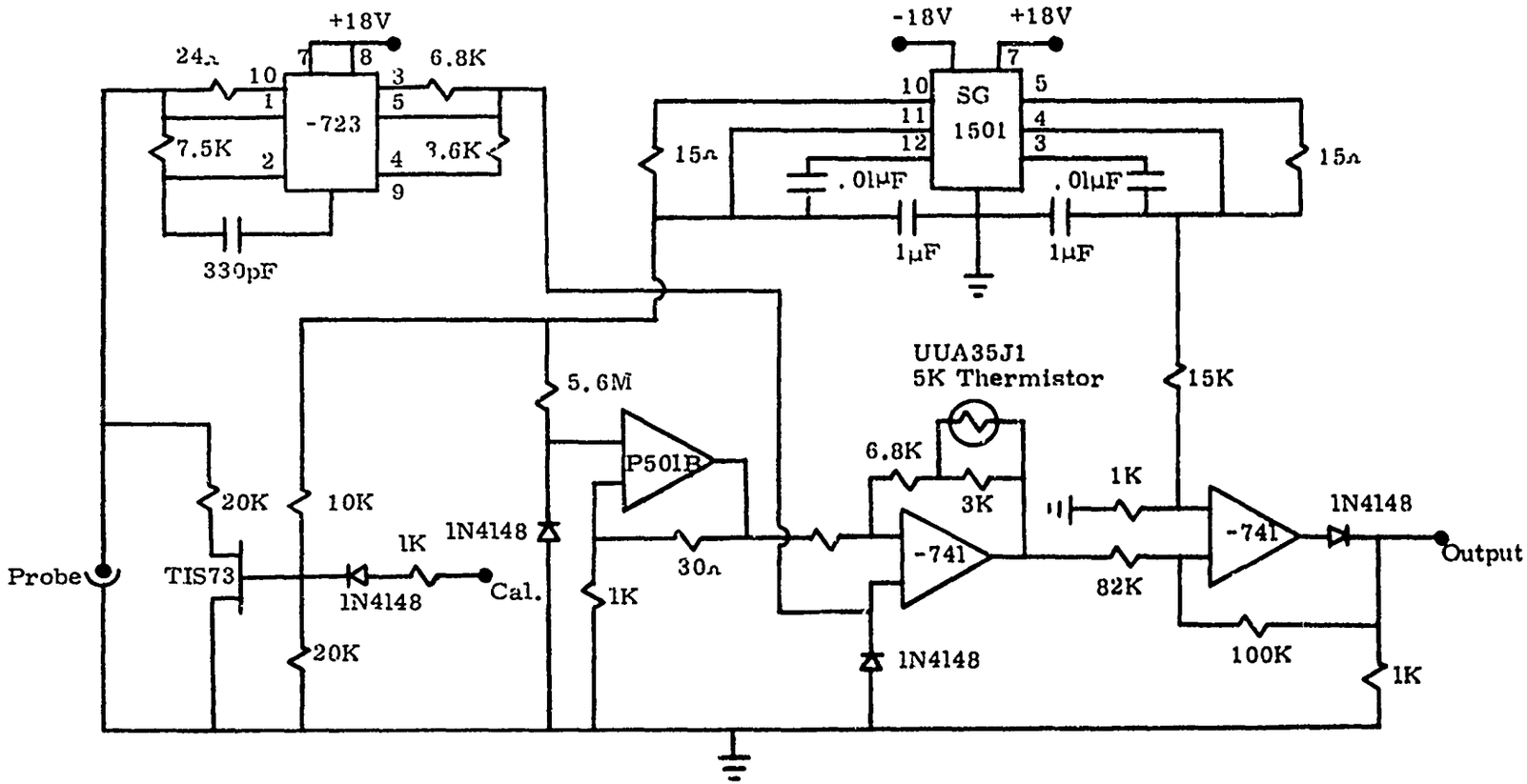

FIGURE 10 FIXED BIAS PROBE CIRCUITS

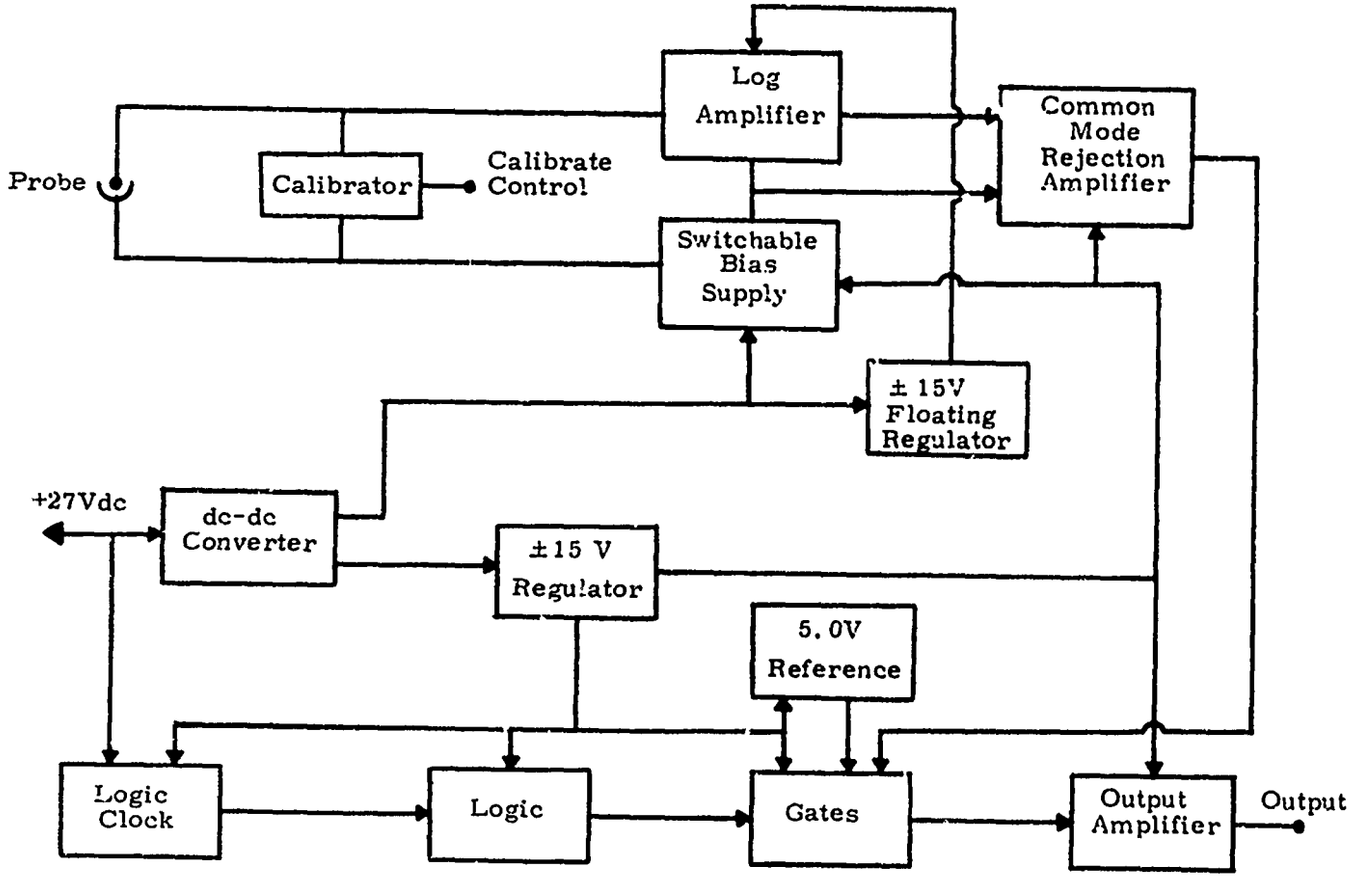

FIGURE 11 VARIABLE BIAS ES-PROBE DIAGRAM

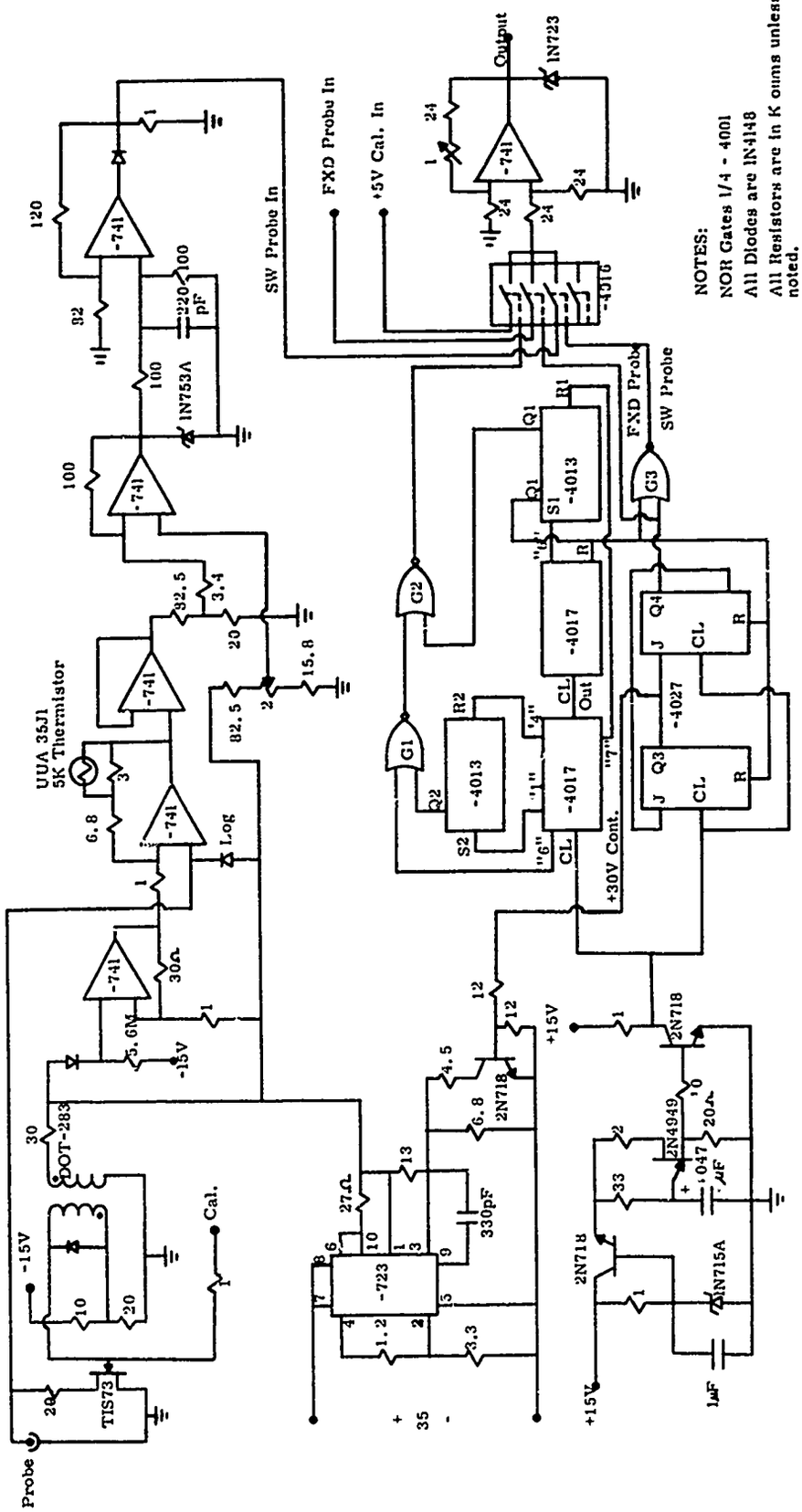

FIGURE 12 VARIABLE BIAS PROBE CIRCUITS

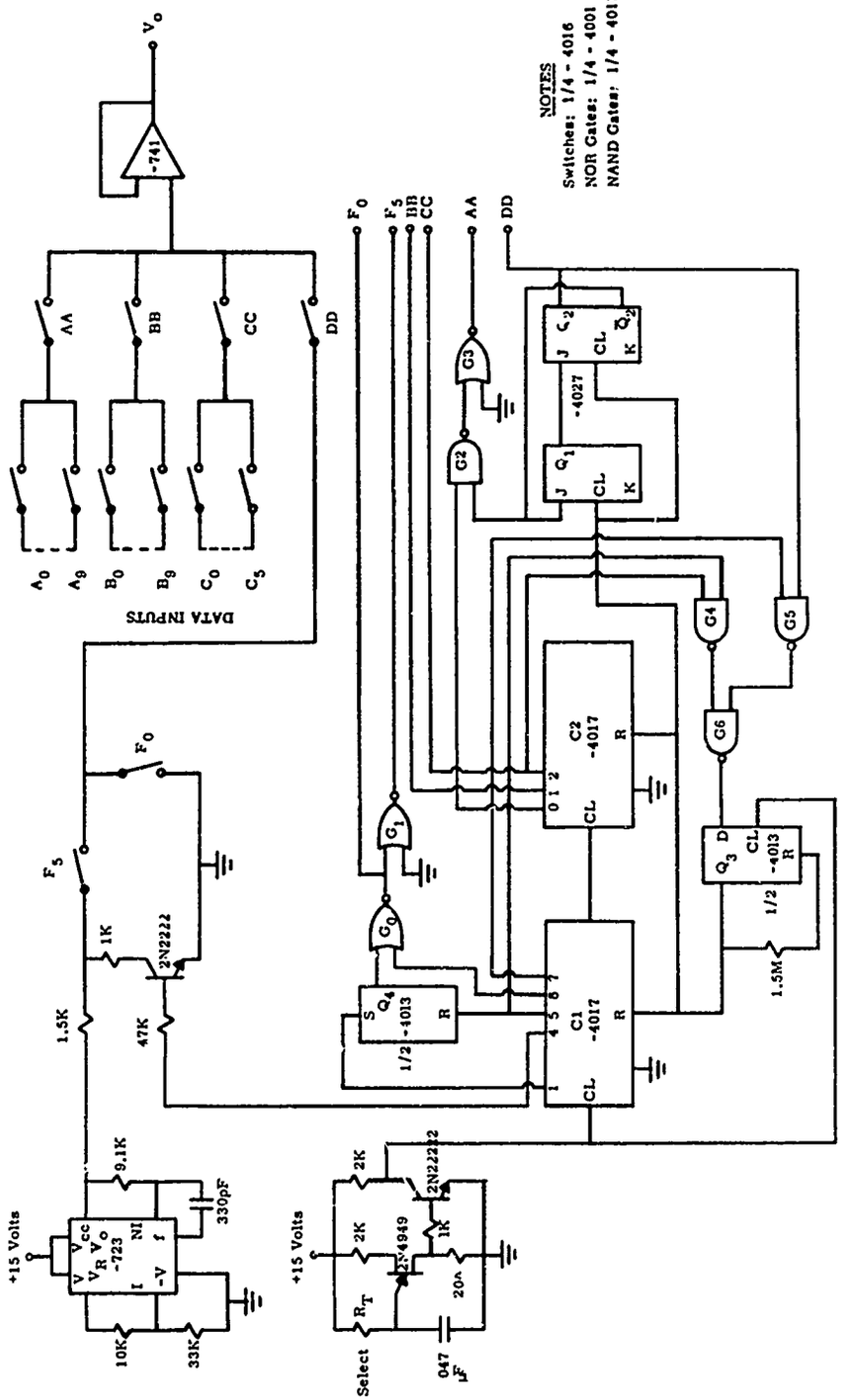

FIGURE 13 COMMUTATOR